

## Synthesis of Cr<sub>2</sub>O<sub>3</sub>/TiO<sub>2</sub> Nanocomposite and its Application as the Blocking Layer in Solar Cells

Fatemeh Talavari<sup>1</sup>, Alireza Shakeri<sup>2</sup> and Hossein Mighani<sup>1\*</sup>

<sup>1</sup>Department of Chemistry, Golestan University, Gorgan, Iran

<sup>2</sup>School of Chemistry, University of Tehran, Tehran, Iran

\*Corresponding author: Hossein Mighani, Department of Chemistry, Golestan University, Gorgan, Iran, Tel: +981732245964; E-mail: h.mighani@gu.ac.ir

Received date: February 14, 2018; Accepted date: February 20, 2018; Published date: February 23, 2018

Copyright: © 2018 Talavari F, et al. This is an open-access article distributed under the terms of the Creative Commons Attribution License, which permits unrestricted use, distribution, and reproduction in any medium, provided the original author and source are credited.

### Abstract

In this study, Cr<sub>2</sub>O<sub>3</sub>/TiO<sub>2</sub> nanoparticles were synthesized using sol-gel method. TiO<sub>2</sub> as one of the most important semiconductor materials with a variety of applications in many fields including photocatalysis and solar cells combined with Cr<sub>2</sub>O<sub>3</sub> as a mineral material and one of the basic oxides used as pigments to improve properties such as mechanical strength, thermal stability form the Cr<sub>2</sub>O<sub>3</sub>/TiO<sub>2</sub> nanocomposite showing attractive applications in photocatalysis and solar cells. To this end, its application in solar cells has been investigated to testify its performance. The results were promising in the case of solar cell. Cr<sub>2</sub>O<sub>3</sub>/TiO<sub>2</sub> nanocomposite solution formed a compact layer with low defects and grain boundaries while it was sprayed as blocking layer (TiO<sub>2</sub>) in superstrate structure CZTS solar cells (Glass/FTO/TiO<sub>2</sub>/In<sub>2</sub>S<sub>3</sub>/CZTS/carbon). Compared to individual TiO<sub>2</sub> blocking layer, the as-deposited layer showed better quality and performance. X-Ray was used to confirm synthesized nanoparticles and their morphology was investigated by Field-Emission Scanning Electron Microscopy (FE-SEM).

**Keywords:** Solar cells; Nanocomposite; Nanoparticles; Blocking layer

### Introduction

Semiconducting materials are of high interest for their attractive applications in fields of photocatalysis and solar cells [1]. CZTS solar cells are promising alternatives to the conventional high cost silicon solar cells and their counterparts CIGS solar cells [2]. CZTS solar cells are made of Copper, Zinc, Tin and Sulfide/Selenide as their raw materials which are abundant elements in earth crust with lower cost compared to CIGS solar cell's raw materials of Indium and Gallium [3]. Thus, it is highly desirable to improve the efficiency of low cost CZTS solar cells. One way to improve the efficiency of such solar cells is modifying different layers including the blocking layer made of up TiO<sub>2</sub> which acts as an electron transporter and as a barrier to prevent the cell from getting short-circuited [4,5]. Having large grain boundaries and many defects which is the main causes of electron hole recombination, makes TiO<sub>2</sub> an undesired choice for having an efficient solar cell for the future market and opens the way for a quest to find new materials as the alternatives although TiO<sub>2</sub> is the most widely used material in solar cells including provskite and other thin film solar cells [6]. There has been many works done by the others in the literature which describes the best effect of a high quality blocking layer on the performance of solar cells. Among previews works on modification of TiO<sub>2</sub> blocking layer, Alexander Agrios reported an improvement in charge transfer by synthesizing a nanocomposite of ZnO/TiO<sub>2</sub> used in dye sensitized solar cells which they showed a different application of such nanocomposites as the blocking layer [7]. Other works include synthesis of such nanocomposites by Keisuke Kawata using polymers like polyaniline as the additive material to TiO<sub>2</sub> to make it a better electron transporter in dye sensitized solar cells [8]. To best of our knowledge, there hasn't been any report in the literature about the application of such nanocomposites in inorganic solar cells of CZTS or CIGS. Thin film inorganic semiconductor of Cr<sub>2</sub>O<sub>3</sub> has a wide variety

of features including: high thermal stability and mechanical strength with low friction coefficient [9]. Cr<sub>2</sub>O<sub>3</sub> nanoparticles could be prepared in different sizes using different techniques including: sol-gel method [10], gas condensation [11], microwave plasma [12] with a variety of morphologies like thin films [13], porous microspheres [14], nanowires [15], nanotubes [16] and so on. Among all of these synthesis processes and morphologies, only few researches have been doing on the synthesis of round shape Cr<sub>2</sub>O<sub>3</sub> nanoparticles ranging from 5 to 200 nm which has the potential to be used as spraying materials having significant features like high temperature resistance which is very important factor in solar cells as well as corrosion resistance, wear resistance features which are beneficial in other applications [17,18]. Semiconductor TiO<sub>2</sub> is a low cost, non-toxic material with a wide range of applications in solar cells [19,20], photocatalyst [21-23], sensors [24,25] etc. which is readily available. Having a band gap of 3.2 eV, TiO<sub>2</sub> could be largely used in solar cells and photocatalysts [26]. Among the photocatalyst materials, synthesis of these two nanoparticles as combined materials, a nanocomposite of TiO<sub>2</sub>/Cr<sub>2</sub>O<sub>3</sub> forms which has different attractive characteristics for solar cell and photocatalytic applications [27].

In this work, we synthesized nanocomposite powder of TiO<sub>2</sub>/Cr<sub>2</sub>O<sub>3</sub> using sol gel method. Following SEM images, the synthesized powder showed good homogeneity with nanoparticles having an average size of about 35 nm. The as-prepared nanocomposite was used to evaluate its performance in photocatalytic and solar cell applications. To testify its performance in solar cells, we sprayed 4 ml of the solution on Fluorine-doped Tin Oxide (FTO) with water as the solvent at 450°C. The as-deposited layer was shown to be a compact layer with lower defects compared to TiO<sub>2</sub> which is always regarded as a layer full of defects effecting charge transfer due to high rate of electron recombination in grain boundaries and defects. To the best of our knowledge, this synthesized nanocomposite shows to be a promising alternative to its counterpart semiconductors with the same

applications especially in solar cells with the big issue of having blocking layers with much grain boundaries and defects.

## Experimental

### Materials

Cr(NO<sub>3</sub>)<sub>2</sub>·6H<sub>2</sub>O with molecular weight 291 g/mol, Ethanol, Acetyl Acetone and Ethylene Glycol (EG), Tetra iso-Propyl Ortho Titanat (TPOT) with chemical formula C<sub>12</sub>H<sub>28</sub>O<sub>4</sub>Ti, density of 0.967 kg/l and MW of 284.66 g/mol were purchased from Merck company.

### Synthesis method

According to calculations carried out beforehand, for the preparation of 5 g of the desired nanoparticles, 6.402 g of Cr(NO<sub>3</sub>)<sub>2</sub>·6H<sub>2</sub>O was weighed, then 3 ml Ethanol was added to the container and placed in the ultrasonic water bath for 5 min, then, after adding 3 ml Acetyl acetone it was left in the ultrasonic bath for 10 min, in the third stage, 6.15cc EG was added and ultrasonicated until the complete dissolution of color of Cr(NO<sub>3</sub>)<sub>2</sub>·6H<sub>2</sub>O in the solution. At the end of this phase, the black was changed into aura green. In the end, as the most important step, 8.19 ml TPOT was added to the container and left for 30 min in ultrasonic bath.

In the next step, container was left in the oven at 65°C until it was transformed from gel phase into solid phase. After leaving the oven, the final product was crushed in a mortar and put in a furnace following a temperature program. After leaving the furnace, the green color of final product showed to be the initial sign of Cr<sub>2</sub>O<sub>3</sub>/TiO<sub>2</sub> nanoparticles synthesized [28].

### Characterization and property measurements

XRD patterns to analyze crystal structure of powders were recorded on X-Ray diffractometer (STOE-STADV) using Cu K $\alpha$  radiation ( $\lambda=1.5408$ ). Surface morphology and sizes of products were performed by (FE-SEM).

### Fabrication of solar cells

To testify the application prepared nanocomposite, we examined the superstrate CZTS solar cell structure (Figure 1) as an inorganic thin film solar cell, one of the candidates to replace high cost CIGS solar cells. The whole fabrication procedure was done following former works in the literature [29]. A solution of these nanocomposites was prepared using non-toxic solvent of water to assure the safety of spray pyrolysis process following previews works in the literature. The FTO substrate was annealed up to 450°C and the solution was sprayed on the substrate using 4 ml of solution [30]. This was repeated for three times and the quality of the layer was examined by FE-SEM.

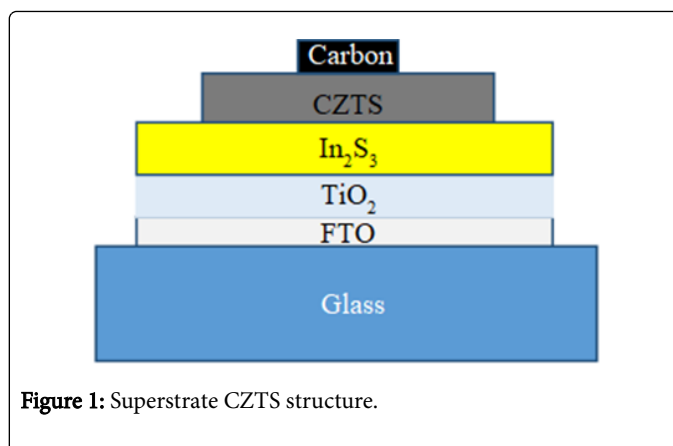


Figure 1: Superstrate CZTS structure.

## Results and Discussion

All diffraction peaks of Figure 2 can be indexed to those of pure rhombohedral phase Cr<sub>2</sub>O<sub>3</sub> (JCPDS No. 38-1479), and the sharp peaks reveal that the products are well crystallized Cr<sub>2</sub>O<sub>3</sub>/TiO<sub>2</sub>, Cr<sub>2</sub>O<sub>3</sub>, TiO<sub>2</sub> nanoparticles. By comparing the XRD pattern of nanopowder with XRD patterns of nanoparticles TiO<sub>2</sub> and also Cr<sub>2</sub>O<sub>3</sub>, the formation of Cr<sub>2</sub>O<sub>3</sub>/TiO<sub>2</sub> has been confirmed by Table 1.

2 $\theta$	FWHM	$\beta$ (°)	D (nm)	Identification product
24.53	0.36	0.00626	22.69	Cr <sub>2</sub> O <sub>3</sub>
26.33	0.24	0.004176	34.15	Cr <sub>2</sub> O <sub>3</sub>
27.53	0.24	0.0047	34.24	TiO <sub>2</sub> -rutile
33.61	0.36	0.00626	23.5	Cr <sub>2</sub> O <sub>3</sub>
36.13	0.24	0.004176	35.03	Cr <sub>2</sub> O <sub>3</sub>
37.12	0.18	0.003132	46.84	New product
39.19	0.24	0.004176	35.28	New product
41.27	0.36	0.00626	23.62	TiO <sub>2</sub> -rutile
42.91	0.18	0.003132	47.58	New product
44.05	0.24	0.004176	35.83	TiO <sub>2</sub> -rutile

Table 1: Results of X-Ray spectroscopy.

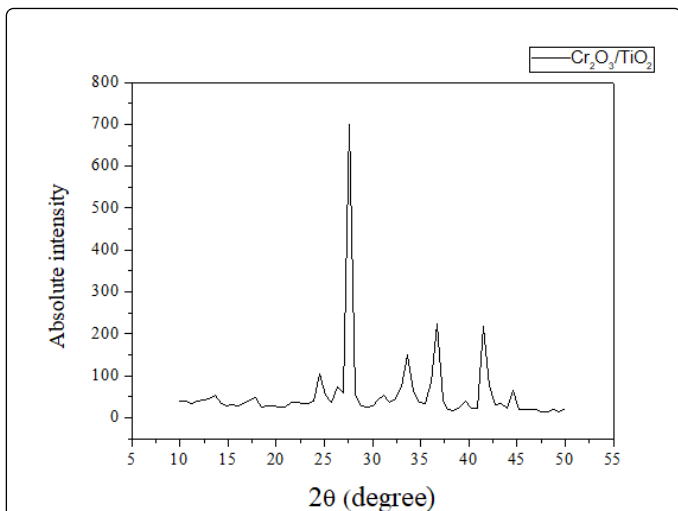


Figure 2: Powder X-Ray diffraction patterns of Cr<sub>2</sub>O<sub>3</sub>/TiO<sub>2</sub>.

Figure 3 shows the IR spectra of (a) Cr<sub>2</sub>O<sub>3</sub> sphere and (b) Cr<sub>2</sub>O<sub>3</sub>/TiO<sub>2</sub> composite sphere. The peaks observed at 529.46 cm<sup>-1</sup>, 589.24 cm<sup>-1</sup> and 1602.16 cm<sup>-1</sup> confirmed the formation of Cr<sub>2</sub>O<sub>3</sub>. Cr<sub>2</sub>O<sub>3</sub>/TiO<sub>2</sub> showed the peaks at 852.7 cm<sup>-1</sup> and 913.18 cm<sup>-1</sup>. The peaks observed at 3419.99 cm<sup>-1</sup> probably represent TiO<sub>2</sub>.

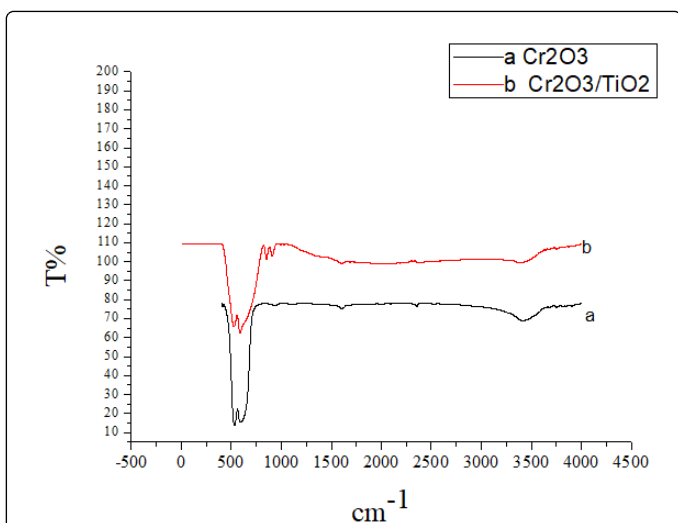


Figure 3: IR spectra of (a) Cr<sub>2</sub>O<sub>3</sub> sphere (b) Cr<sub>2</sub>O<sub>3</sub>/TiO<sub>2</sub> composite sphere.

### Solar cell application

The morphology of the resulting powder was examined by FE-SEM. The FE-SEM micrograph in Figure 4 shows the morphology of as-synthesized Cr<sub>2</sub>O<sub>3</sub>/TiO<sub>2</sub> nanopowder, revealing uniform spherical shapes and very small particles of nanosize. The calculated average particle size of Cr<sub>2</sub>O<sub>3</sub>/TiO<sub>2</sub>, Cr<sub>2</sub>O<sub>3</sub>, TiO<sub>2</sub> was 35 nm with a standard deviation of ± 13 nm, and consistent with the aforementioned size calculated by Scherrer's relation.

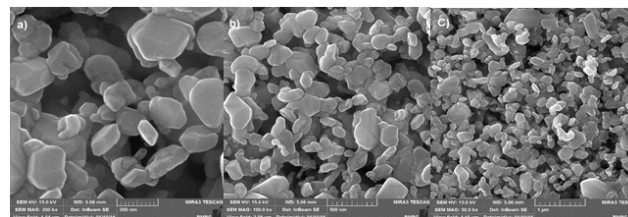


Figure 4: FE-SEM top view of Cr<sub>2</sub>O<sub>3</sub>/TiO<sub>2</sub> nanoparticles: a) 200 nm b) 500 nm c) 1 μm.

Nanocomposite of TiO<sub>2</sub>/Cr<sub>2</sub>O<sub>3</sub> could be used as a precursor solution in water to be sprayed as the blocking layer in photovoltaic applications [31]. The role of blocking layer is very crucial in solar cells as it acts both as an electron transporter by aligning its band gap with the top layers and as a barrier to prevent the solar cell from getting short circuited as the top layers could penetrate through the bottom layers during the deposition process [32]. Having an optimum band gap of 3.2 eV, it is highly desirable to use it as blocking layer. The final deposited layer showed very compact, low defect islands under FE-SEM with a thickness of 120 nm to be favorable for electron transfer. As shown in Figure 4, this compact layer seems promising to be an alternative to the TiO<sub>2</sub> blocking layer as it is obvious that TiO<sub>2</sub>/Cr<sub>2</sub>O<sub>3</sub> nanocomposite forms a dense blocking layer with lower defects and grain boundaries compared to individual TiO<sub>2</sub> deposited layer as shown in Figure 5. To evaluate its performance we made CZTS superstrate solar cells using this compact layer as the blocking layer. The results were promising with an improvement in the efficiencies followed by an enhancement in J<sub>sc</sub> and constant V<sub>oc</sub>. Fill factor decreases as a result of increasing current. The results are shown in Table 2. The J-V curve for the best cell is shown in Figure 6.

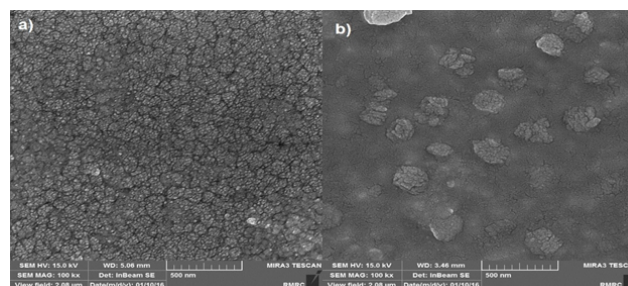


Figure 5: FE-SEM images of a) TiO<sub>2</sub> sprayed at 450°C b) TiO<sub>2</sub>/Cr<sub>2</sub>O<sub>3</sub> nanocomposite sprayed at 450°C.

Blocking layer	V <sub>oc</sub> (volt)	J <sub>sc</sub> (mA.cm <sup>-2</sup> )	FF (%)	Eff (%)
TiO <sub>2</sub>	0.35	4.65	43	0.7
TiO <sub>2</sub> /Cr <sub>2</sub> O <sub>3</sub>	0.35	9.2	33	1.07

Table 2: A comparison on the effect of two different blocking layers on CZTS solar cells.

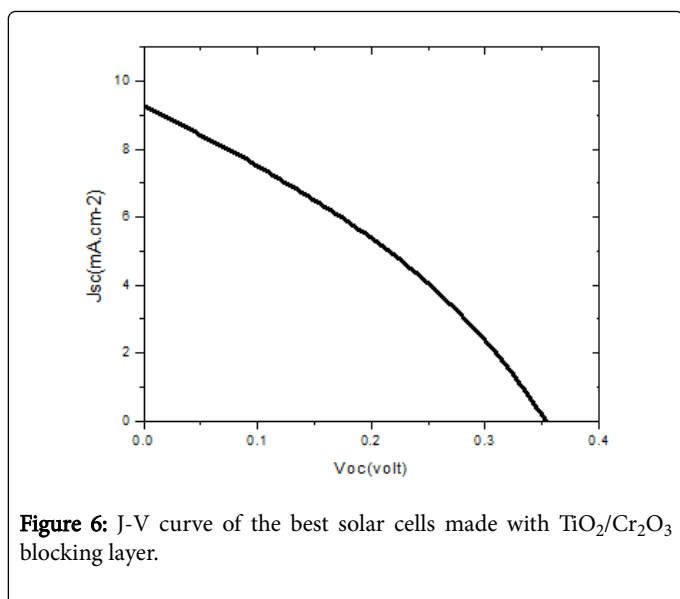


Figure 6: J-V curve of the best solar cells made with TiO<sub>2</sub>/Cr<sub>2</sub>O<sub>3</sub> blocking layer.

## Conclusion

In this study Cr<sub>2</sub>O<sub>3</sub>/TiO<sub>2</sub> nanoparticles were investigated with a new technique from sol-gel method by using Cr(NO<sub>3</sub>)<sub>2</sub>·6H<sub>2</sub>O and TPOT synthesized Cr<sub>2</sub>O<sub>3</sub>/TiO<sub>2</sub> nanopowder, revealed uniform spherical shapes and very small particles. Investigating application of this nanocomposite in solar cells, it reveals that it has a very high potential to be used in different types of solar cells and boost efficiencies to reach better records in this promising field of energy. Although the new blocking layer slightly improved low efficient superstrate CZTS solar cells, noticing the fact that CZTS solar cells are half efficient compared to provskite solar cells it can be interpreted that using such low defect blocking layer in provskite solar cells with TiO<sub>2</sub> blocking layer could improve the efficiencies more than it was shown here.

## Acknowledgement

We are pleased to thank our colleagues Morteza Saadattalab and Maryam Binabaji with their role of consulting us during the project.

## References

1. Tian Q, Huang L, Zhao W, Yang Y, Wang G, et al. (2015) Metal sulfide precursor aqueous solutions for fabrication of Cu<sub>2</sub>ZnSn (S,Se)<sub>4</sub> thin film solar cells. *Green Chemistry* 17: 1269-1275.
2. Gholami H, Saadattalab V, Shakeri A (2016) Effect of CNTs and nano ZnO on physical and mechanical properties of polyaniline composites applicable in energy devices. *Progress in Natural Science: Materials International* 26: 36046-36052.
3. Pateter A (2015) Investigation on the formation of copper zinc tin sulphide nanoparticles from metal salts and dodecanethiol. *Materials Chemistry and Physics* 149-150: 517-522.
4. Lellig P (2015) Application of hybrid blocking layers in solid-state dye-sensitized solar cells. *Springer Plus* 4: 1-8.
5. Guan J, Zhang J, Yu T, Xue G, Yu X, et al. (2012) Interfacial modification of photoelectrode in ZnO-based dye-sensitized solar cells and its efficiency improvement mechanism. *RSC Advances* 2: 7708-7713.
6. Yu H, Zhang S, Zhao H, Xue B, Liu P, et al. (2009) High-performance TiO<sub>2</sub> photoanode with an efficient electron transport network for dye-sensitized solar cells. *The Journal of Physical Chemistry C* 113: 16277-16282.
7. Manthina V, Baena JPC, Liu G, Agrios AG (2012) ZnO - TiO<sub>2</sub> Nanocomposite Films for High Light Harvesting Efficiency and Fast Electron Transport in Dye-Sensitized Solar Cells. *The Journal of Physical Chemistry C* 116: 23864-23870.
8. Kawata K, Gan SN, Ang DTC, Sambasevam KP, Phang SW, et al. (2013) Preparation of polyaniline/TiO<sub>2</sub> nanocomposite film with good adhesion behavior for dye-sensitized solar cell application. *Polym Composites* 34: 1884-1891.
9. Sourty E, Sullivan JL, Bijker MD (2003) Chromium oxide coatings applied to magnetic tape heads for improved wear resistance. *Tribology International* 36: 389-396.
10. Kawabata A, Yoshinaka M, Hirota K, Yamaguchi O (1995) Hot Isostatic Pressing and Characterization of Sol-Gel-Derived Chromium (III) Oxide. *Journal of the American Ceramic Society* 78: 2271-2273.
11. Alrehaily LM, Joseph JM, Wren JC (2015) Radiation-Induced Formation of Chromium Oxide Nanoparticles: Role of Radical Scavengers on the Redox Kinetics and Particle Size. *The Journal of Physical Chemistry C* 119: 16321-16330.
12. Pei Z, Xu H, Zhang Y (2009) Preparation of Cr<sub>2</sub>O<sub>3</sub> nanoparticles via C<sub>2</sub>H<sub>5</sub>OH hydrothermal reduction. *Journal of Alloys and Compounds* 468: L5-L8.
13. Shin JU, Kim DJ, Park SH, Han YT, Sung HK (2002) An Etch-Stop Technique Using Cr<sub>2</sub>O<sub>3</sub> Thin Film and its Application to Silica PLC Platform Fabrication. *ETRI journal* 24: 398-400.
14. Sun H, Wang L, Chu D, Ma Z, Wang A (2015) Synthesis of porous Cr<sub>2</sub>O<sub>3</sub> hollow microspheres via a facile template-free approach. *Materials Letters* 140: 35-38.
15. Yang S (2012) Single crystalline Cr<sub>2</sub>O<sub>3</sub> nanowires/nanobelts: CrCl<sub>3</sub> assistant synthesis and novel magnetic properties. *Applied Surface Science* 258: 8965-8969.
16. Zhang XZ, Han D, He YB, Zhai DY, Liu D, et al. (2015) Mesoporous Cr<sub>2</sub>O<sub>3</sub> nanotubes as an efficient catalyst for Li-O<sub>2</sub> batteries with low charge potential and enhanced cyclic performance. *Journal of Materials Chemistry A* 4: 7727-7735.
17. Singh H, Grewal MS, Sekhon HS, Rao RG (2008) Sliding wear performance of high-velocity oxy-fuel spray Al<sub>2</sub>O<sub>3</sub>/TiO<sub>2</sub> and Cr<sub>2</sub>O<sub>3</sub> coatings. *Proceedings of the Institution of Mechanical Engineers, Part J: Journal of Engineering Tribology* 222: 601-610.
18. Ouyang J, Sasaki S (2001) Effects of different additives on microstructure and high-temperature tribological properties of plasma-sprayed Cr<sub>2</sub>O<sub>3</sub> ceramic coatings. *Wear* 249: 56-66.
19. Wang J, Qu S, Zhong Z, Wang S, Liu K, et al. (2014) Fabrication of TiO<sub>2</sub> nanoparticles/nanorod composite arrays via a two-step method for efficient dye-sensitized solar cells. *Progress in Natural Science: Materials International* 24: 588-592.
20. Frank AJ, Kopidakis AN, Lagemaat JVD (2004) Electrons in nanostructured TiO<sub>2</sub> solar cells: transport, recombination and photovoltaic properties. *Coordination Chemistry Reviews* 248: 1165-1179.
21. Nakata K, Fujishima A (2012) TiO<sub>2</sub> photocatalysis: Design and applications. *Journal of Photochemistry and Photobiology C: Photochemistry Reviews* 13: 169-189.
22. Pan L, Huang H, Lim CK, Hong QY, Tse MS (2013) TiO<sub>2</sub> rutile-anatase core-shell nanorod and nanotube arrays for photocatalytic applications. *RSC Advances* 3: 3566-3571.
23. El-Roz M, Haidar Z, Lakiss L, Toufaily J, Thibault-Starzyk F (2013) Immobilization of TiO<sub>2</sub> nanoparticles on natural Luffa cylindrical fibers for photocatalytic applications. *RSC Advances* 3: 3438-3445.
24. Bai J, Zhou B (2014) Titanium Dioxide Nanomaterials for Sensor Applications. *Chemical Reviews* 114: 10131-10176.
25. Cui S, Wang J, Wang X (2015) Fabrication and design of a toxic gas sensor based on polyaniline/titanium dioxide nanocomposite film by layer-by-layer self-assembly. *RSC Advances* 5: 58211-58219.
26. Valencia S, Marin JM, Restrepo G (2009) Study of the Bandgap of Synthesized Titanium Dioxide Nanoparticles Using the Sol-Gel Method

- 
- and a Hydrothermal Treatment. *The Open Materials Science Journal* 4: 9-14.
27. Trache R, Berger LM, Saaro S, Lima RS, Marple BR (2010) The Influence of Particle Temperature, Particle Velocity and Coating Surface Temperature on the Sliding Wear Performance of TiO<sub>2</sub>-Cr<sub>2</sub>O<sub>3</sub> Coatings. *ITSC*.
28. Moghiminia S, Farsi H, Raissi H (2014) Comparative optical and electrochemical studies of nanostructured NiTiO<sub>3</sub> and NiTiO<sub>3</sub>-TiO<sub>2</sub> prepared by a low temperature modified Sol-Gel route. *Electrochimica Acta* 132: 512-523.
29. Lee D, Yong K (2014) Solution-processed Cu<sub>2</sub>ZnSnS<sub>4</sub> superstrate solar cell using vertically aligned ZnO nanorods. *Nanotechnology* 25: 065401.
30. Dehghani M, Behjat A, Tajabadi F, Taghavinia N (2015) Totally solution-processed CuInS<sub>2</sub> solar cells based on chloride inks: reduced metastable phases and improved current density. *Journal of Physics D: Applied Physics* 48: 115304.
31. Manthina V, Agrios AG (2015) Blocking layers for nanocomposite photoanodes in dye sensitized solar cells: Comparison of atomic layer deposition and TiCl<sub>4</sub> treatment. *Thin Solid Films* 598: 54-59.
32. Peng B, Jungmann G, Jäger C, Haarer D, Schmidt HW, et al. (2004) Systematic investigation of the role of compact TiO<sub>2</sub> layer in solid state dye-sensitized TiO<sub>2</sub> solar cells. *Coordination Chemistry Reviews* 248: 1479-1489.